Geosystems and Geoenvironment 2 (2023) 100139

Contents lists available at ScienceDirect

Geosystems and Geoenvironment

journal homepage: www.elsevier.com/locate/geogeo

Insights into the Tethyan mantle heterogeneity: Trace element evidence from the Karakaya Complex, Central Anatolia

Kaan Sayit

Department of Geological Engineering, Middle East Technical University, Ankara 06800, Turkey

ARTICLE INFO

Article history:
Received 3 June 2022
Revised 26 August 2022
Accepted 28 September 2022

Keywords:
FOZO
Mantle geochemistry
Mantle plume
Metasomatism
Tethys

ABSTRACT

The Nilüfer Unit of the Karakaya Complex (northern Turkey) preserves the remnants of the voluminous Triassic Tethyan magmatism. In the Imrahor area (Ankara), the Nilüfer Unit is characterized by a megablock consisting of hydrothermally altered basalts, gabbros, and subordinate wehrlitic cumulates. These lithologies display marked positive Nb anomalies with depleted Th/La ratios and varying degrees of LREE enrichment. They can be subdivided into two groups based on Nb/Nb*, which are not related to each other via fractional crystallization or extent of partial melting. With their strong Nb-kick and broad La/Sm range, the Imrahor lithologies are more akin to FOZO (Focus Zone)- or C (common component)-type melts than EM (Enriched Mantle) and HIMU (high μ). The Zr-Nb systematics reveals that melt mixing was an essential process in the petrogenesis of these mafic rocks. Based on geochemical modeling, the trace element systematics of the İmrahor lithologies can be explained by melting metasomatized oceanic lithospheric mantle (OLM) infiltrated by very low-degree melt fractions. The metasomatized OLM may represent a recycled, plume-related material that has generated Nb-enriched melts during the Triassic Tethyan magmatism.

1. Introduction

The Earth's mantle is made up of distinct domains existing at various scales, with different depletion/enrichment histories (e.g., Zindler and Hart, 1986; Warren et al., 2016). Apart from the major differentiation processes in the early Earth, the heterogeneity of the mantle can be principally attributed to the subduction of slabs into the mantle, and mass fluxes driven by deep-sourced mantle plumes. Delamination of the continental lithosphere is another mechanism that may add heterogeneity to the shallow and deep mantle (e.g., McKenzie and O'Nions, 1983). Partial melts derived from subducted slabs and asthenospheric mantle (possibly from low-velocity zone – LVZ) may also introduce heterogeneities to the continental and oceanic lithospheric mantle (e.g., Sun and McDonough, 1989). In addition, lower mantle melts/residues can be integrated into mantle plumes, thus contributing the mantle heterogeneity (Collerson et al., 2010). After their formation, these heterogeneities are tapped by the partial melts of asthenospheric and lithospheric mantle domains in different tectonic settings.

The recycled/deep-sourced materials have been essential in creating mantle heterogeneity and their origins have been commonly linked to mantle plumes (e.g., Hofmann and White, 1982; Hart et al., 1992; Hanan and Graham, 1996), whose roots might be located in the large, low-velocity regions in the lower mantle (e.g., Burke and Torsvik, 2004). Although this phenomenon is well evidenced by the recent mafic magmatism; tracking the mantle sources and understanding of mantle heterogeneity of ancient magmatic events may not be straightforward as the modern analogs. This is because the old magmatic suites are generally disrupted during the closure of the oceanic domains (e.g., Marroni et al., 2020). In such cases, fragments of igneous-derived lithologies, as the tracers of magmatism, can be preserved in the mélanges and subduction/accretion complexes (e.g., Parlak and Robertson, 2004; Festa et al., 2010; Shervais, 2006; Sayit et al., 2017; Saccani et al., 2018).

The Tethyan realm, as an ancient example, is thought to have involved mantle plumes (e.g., Wilson and Guiraud, 1998; Lapierre et al., 2004; Sayit, 2013). However, in spite of numerous studies attesting to the influence of mantle plumes on the Tethyan magmatism, the understanding of how plume-derived components have contributed to mantle heterogeneity is poorly understood. In this regard, the Nilüfer Unit of the Karakaya Complex (northern Turkey) may provide critical information as it holds the relicts of widespread Triassic within-plate magmatism inherited from

E-mail address: ksayit@metu.edu.tr

https://doi.org/10.1016/j.geogeo.2022.100139

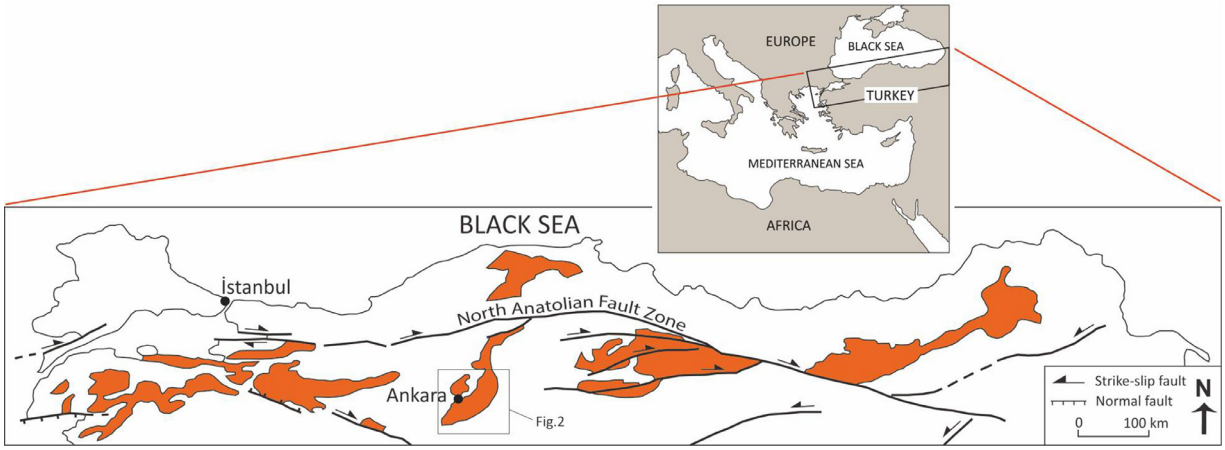

Fig. 1. Distribution of the Sakarya Composite Terrane in Turkey (after Göncüoglu, 2018).

the destruction of the Palaeotethyan lithosphere (e.g., Pickett and Robertson, 1996; Okay, 2000; Sayit and Göncüoglu, 2013). In this study, I revisit the Imrahor area (Ankara, Turkey) in light of new geochemical data, where the Triassic mafic/ultramafic lithologies of the Nilüfer Unit are contained in a megablock within a clastic mélange matrix. These and mafic/ultramafic lithologies show ocean-island basalt (OIB) and enriched mid-ocean ridge basalt (E-MORB)-like signatures with strong enrichment in Nb (relative to Th and La); thus, they can deliver essential information about the recycled/deep-sourced components in the Tethyan sublithospheric mantle. Accordingly, I aim to shed light on the heterogeneity of the Tethyan mantle, particularly concerning the potential role of the metasomatized oceanic lithospheric mantle.

2. Geological overview

Turkey, as a part of the Eastern Mediterranean region, has a complex tectonic framework, which has been mainly achieved through multiple episodes of subduction and collisional orogenesis due to the closure of the Tethyan oceans (e.g., Şengör and Yılmaz, 1981). As a result, Turkey consists of several terranes of Eurasian or Gondwanan affinity, reflecting diverse tectonic histories (Göncüoglu et al., 1997). The present-day terrane distribution of the Anatolian region was obtained after the Alpine Orogeny, following the closure of Neotethyan oceanic domains. The Sakarya Composite Terrane (Fig. 1), one of the Alpine terranes of Turkey, includes a Variscan Paleozoic basement cut by Devonian-Carboniferous granitoids (e.g., Göncüoglu, 2019). This assemblage is tectonically associated with the Karakaya Complex, a Cimmeride unit thought to preserve the remnants of the Palaeotethyan events.

The Karakaya Complex has a wide distribution in Turkey as an E-W trending belt (Okay and Göncüoglu, 2004). It is made up of variably deformed and metamorphosed rock assemblages, consisting chiefly of mafic lithologies, clastic sediments, and limestone. The Karakaya Complex is unconformably overlain by the Liassic sediments (Altiner et al., 1991). The Complex is made up of two major lithological components; (i) mafic unit called the Nilüfer Unit (sensu Sayit et al., 2010), (ii) clastic-dominated unit named the Eymir Unit (Sayit et al., 2011). The Nilüfer Unit consists predominantly of variably metamorphosed mafic igneous rocks associated with volcaniclastic rocks, limestone, mudstone, and chert.

The study area is located in Imrahor (Ankara, Turkey), lying at the central sector of the Nilüfer Unit (Fig. 2). Although the Imrahor area was previously included in the study of Sayit and Göncüoglu (2009), the sampling on this particular locality remained limited since these authors studied a vast region in Central and NW Anatolia. The present study, however, directly targets the Imrahor megablock, with an increasing sampling resolution. In addition, no study before has drawn particular attention to the Nb-enriched nature of these mafic products in the context of the wide-scale Triassic Tethyan magmatism. It must be noted that the sampling was concentrated on the SW part of the megablock, since the NE part does not provide good outcrops due to settlement density.

In the study area, the Karakaya Complex displays a well-developed, block-in-matrix type mélange structure. The mafic lithologies are contained within a megablock, which is in turn enveloped by very low-grade metaclastic rocks of the Eymir Unit. The mafic rocks are characterized chiefly by basalts and, to lesser extent gabbros. Rare ultramafic cumulates are also found. Basalts are the dominant lithology in the study area, and occur in both pillowed and massive forms. They are variably colored with blackish, purplish, and greenish appearance, possibly related to the oxidation and presence of secondary minerals (e.g., chlorite and epidote). In some places, basalts interfinger with volcaniclastic rocks and limestone. Compared to basalts, gabbros are volumetrically minor in the study area. They appear as dark greenish lithologies, with fine- to medium-grained phaneritic texture. In some localities, basalts gradually pass to fine-grained gabbros (diabase), implying that some diabases may represent relatively slowly cooled interior/lower parts of the lava flows. Coarser-grained gabbros, along with wehrlitic cumulates, probably correspond to deeper magmatic levels.

The age of the İmrahor mafic magmatism is Middle Anisian (Middle Triassic), which is tightly constrained by the fossil-bearing limestones intercalated with the basaltic flows (Sayit and Göncüoglu, 2009). The Middle Triassic age also appears to be common for the entire Nilüfer magmatism on the basis of the age findings from other localities (Kaya and Mostler, 1992; Altiner and Kocyigit, 1993; Eyüboglu et al., 2018).

3. Petrography

The Imrahor basalts, gabbros, and wehrlites are all affected by low-grade hydrothermal alteration, and share similar primary and secondary mineralogies. Basalts are generally porphyritic, and to a lesser extent aphyric. Rapidly cooled samples display fine-grained matrix with interstitial glass (now altered), whereas slower cooler rates are characterized by coarser-grained, holocrystalline varieties. Gabbros show fine- to medium-grained phaneritic texture, while wehrlitic ultramafics (cumulates) are medium-grained phaneritic. Clinopyroxene and plagioclase represent the common primary (relict) mineral phases in the Imrahor samples. Kaersutite, as a primary constituent, is also found, but rarely. Clinopyroxene is characterized by brownish- to pinkish-colored, compositionally

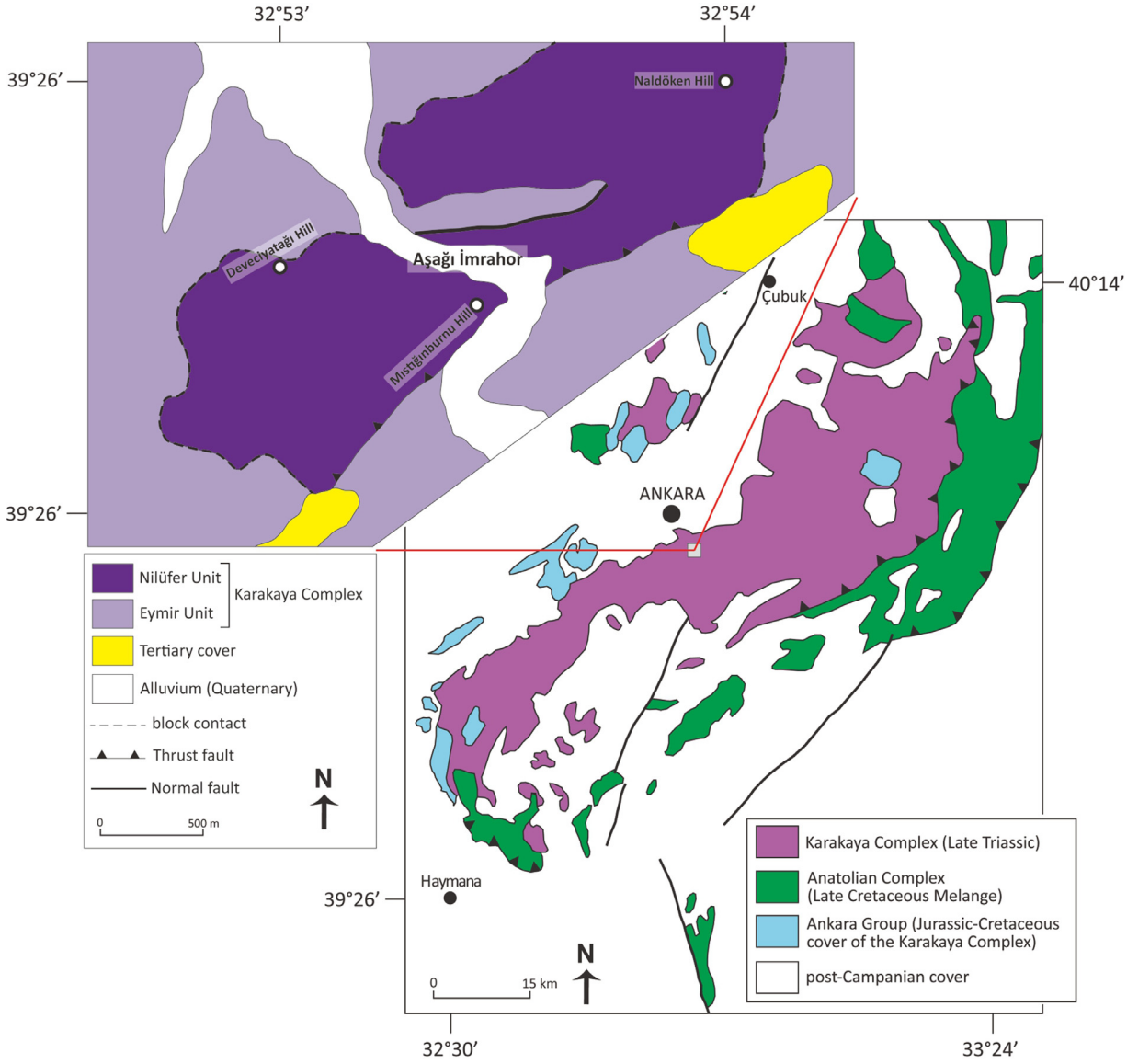

Fig. 2. Geological map the Ankara region and the study area (after Kocyigit, 1991; Sayit and Göncüoglu, 2013).

zoned subhedral crystals of Ti-augite. Twinned grains exist, which can be simple or polysynthetic. Plagioclase occurs mainly as subhedral, lath-shaped grains with polysynthetic twinning. In gabbroic samples, plagioclase laths are associated with larger clinopyroxene grains, forming subophitic texture. In wehrlites, olivine (now pseudomorphed by secondary minerals) occurs as the cumulate phase, whereas plagioclase and clinopyroxene are interstitial phases.

Hydrothermal alteration seems to have occurred under the lower greenschist facies (prehnite-pumpellyite) conditions. Sericitization is common in plagioclase. Chlorite, epidote, prehnite, clays, and calcite are other secondary phases replacing plagioclase. Clinopyroxene is generally altered to chlorite and lesser extent, to calcite. Olivine is totally altered and pseudomorphed by serpentine, chlorite, and calcite. Amygdules, which are common in basalts, include calcite, zeolite, prehnite, epidote, and pumpellyite.

4. Geochemistry

4.1. Analytical method

25 samples collected from the İmrahor area were analyzed for major and trace elements in the Activation Laboratories. The analytical data is given in Supplementary Data (Table S1). In preparation for analyses, samples were fluxed by lithium metaborate and lithium tetraborate fusion, and then fused in an induction furnace. Subsequently, the molten melt was poured into a 5% nitric acid solution with an internal standard, which is performed until a complete dissolution is achieved. Major elements and a subset of trace elements Ba, Sc, Sr, V, Y, and Zr were analyzed by ICP-OES, whereas the rest of trace elements were measured by ICP-MS. Based on the analyses of standards and replicates, accuracy was generally better than 2% for major elements and 7% for trace elements, while reproducibility was generally better than 5% (Supplementary Data, Table S2).

4.2. Assessment of alteration

The influence of hydrothermal alteration on the Imrahor lithologies is also reflected by the chemistry, with high loss on ignition (LOI) values between 4.1 and 12.3 wt.%. It is critical, therefore, to assess to what extent the sample compositions reflect the pristine, unaltered chemistry. It is known that the elements with low and high ionic potentials tend to be fluid-mobile (e.g., K, Rb, Si; Pearce, 1975). On the other hand, the elements with rather mod-

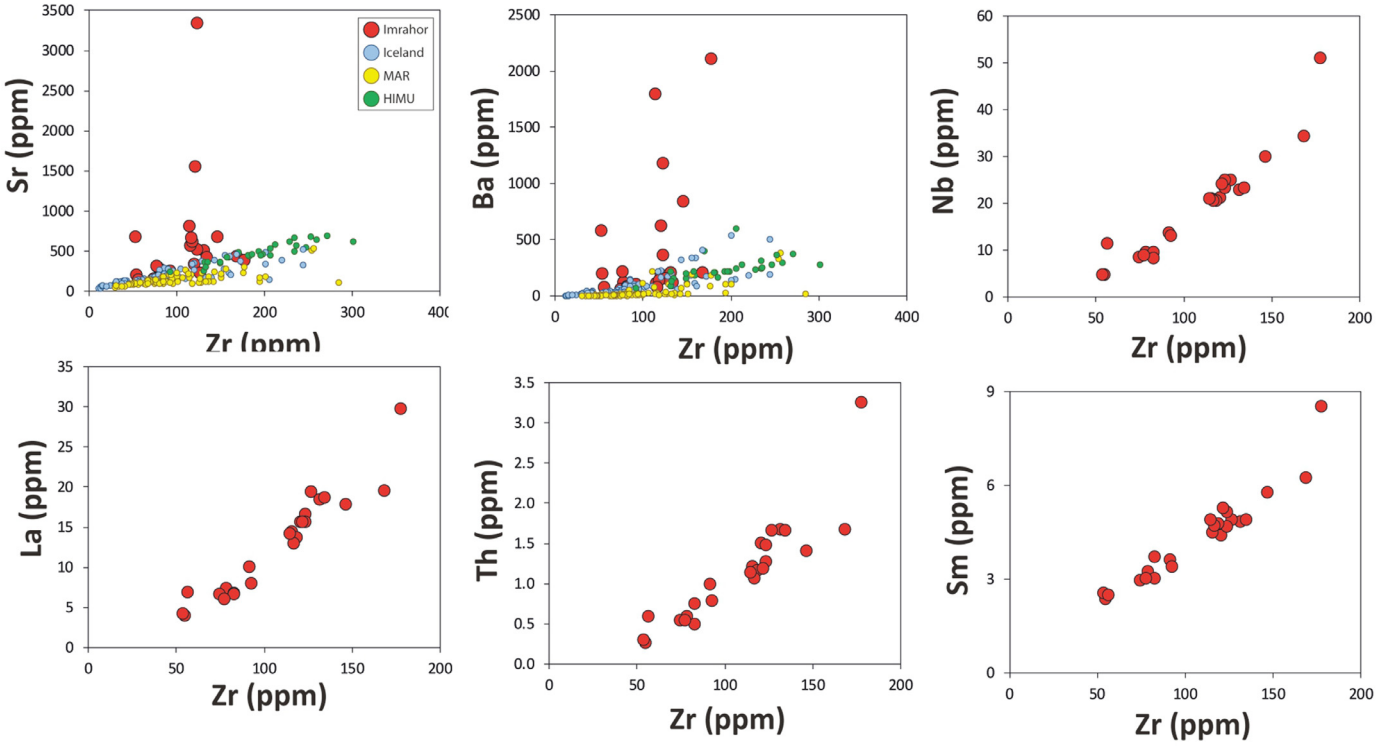

Fig. 3. Plots of selected trace elements versus Zr for the assessment of mobility. Note the erratic distribution and anomalously high values of Sr and Ba in the İmrahor basalts and gabbros (and a wehrlite) from the Nilüfer Unit, indicating their mobility. This contrast with the linear trends observed in the East Pacific Rise (EPR; 5-15°N; Niu and Batiza, 1997), Iceland (Kokfelt et al., 2006) and HIMU islands (Woodhead, 1996; Hanyu et al., 2011), where these elements have remained immobile.

erate ionic potentials (e.g., high-field strength elements – HFSE and REE; e.g., Th, Zr, La, Yb) are relatively immobile during alteration/metamorphism (e.g., Bach et al., 2003). For the Imrahor samples, the so-called fluid-mobile elements (e.g., Ba and K) display no correlation with Zr (a highly stable element during low-grade alteration), whereas HFSE and REE are strongly positively correlated (including also the samples with very high LOI; Fig. 3). This suggests that HFSE and REE have remained immobile against hydrothermal alteration. This conclusion is also supported by multi-element plots, in which HFSE and REE show parallel/sub-parallel patterns, which would be difficult to obtain if they were mobilized through variable volatile influx (as indicated by a broad spectrum in LOI). In contrast, low-ionic potential elements show highly inconsistent behavior, which can be attributed to their variable loss or gain during water-rock interaction. Hence, in making the petrogenetic interpretations, the main emphasis will be on the HFSE and REE, whose abundances reflect the pristine chemistry.

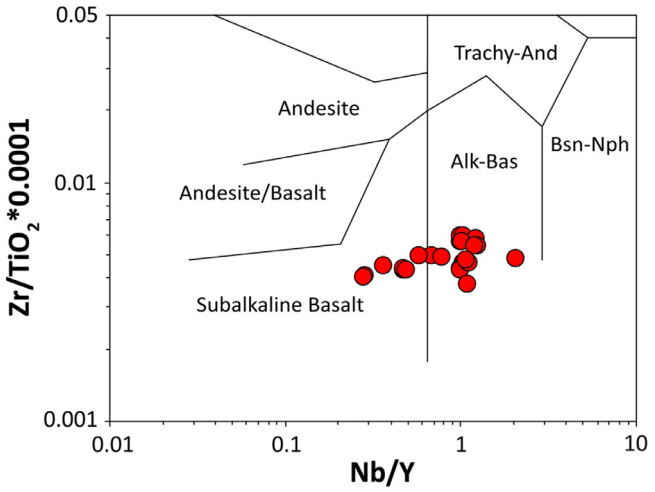

Fig. 4. Chemical classification of the İmrahor basalts and gabbros (after Winchester and Floyd, 1977). Note that although it is ultramafic, the wehrlitic sample (15-IM-22A) is also included in the plot to display its alkalinity.

4.3. Results

Alkalies and silica appear to have been mobilized in the samples. Thus, the immobile element-based scheme of Winchester and Floyd (1977) is preferred here instead of 'total alkali vs silica diagram'. The plot reveals that all samples are basaltic in composition (except wehrlite), with both tholeiitic and alkaline varieties (Fig. 4). For basalts and gabbros, the samples have a wide range of MgO between 3.2-11.2 wt.%, whereas the wehrlite sample has 25.3 wt.% MgO, consistent with its cumulate nature. It must be noted that MgO is somewhat influenced by alteration; however, the compositional range mostly seems realistic except for the samples with low MgO (two samples with 3.8 and 4.8 wt.% MgO). These samples also have the highest LOI (with 12.2 and 12.3 wt.%), suggesting that MgO has likely been leached during hydrothermal alteration. Thus, except for these samples, MgO is still useful, consistent with its positive correlation with Ni, Co, and Cr.

On the primitive mantle (PM)-normalized plots (Fig. 5), the Imrahor samples show strong positive Nb anomalies (i.e., Nb-kick), with a wide range of Nb/Nb* values between 1.4 and 2.1 (calculated as $[Th_{PM} \times La_{PM}]^{0.5}$; where PM refers to PM-normalized). It must be noted that Nb/Nb* is not correlated with MgO, suggesting that the level of Nb-kick is not controlled by fractional crystallization. To better monitor the influence of Nb-kick on the petrogenesis of Imrahor lithologies, the samples were arbitrarily divided into two groups, namely Group 1 with Nb/Nb* between 1.42-1.69

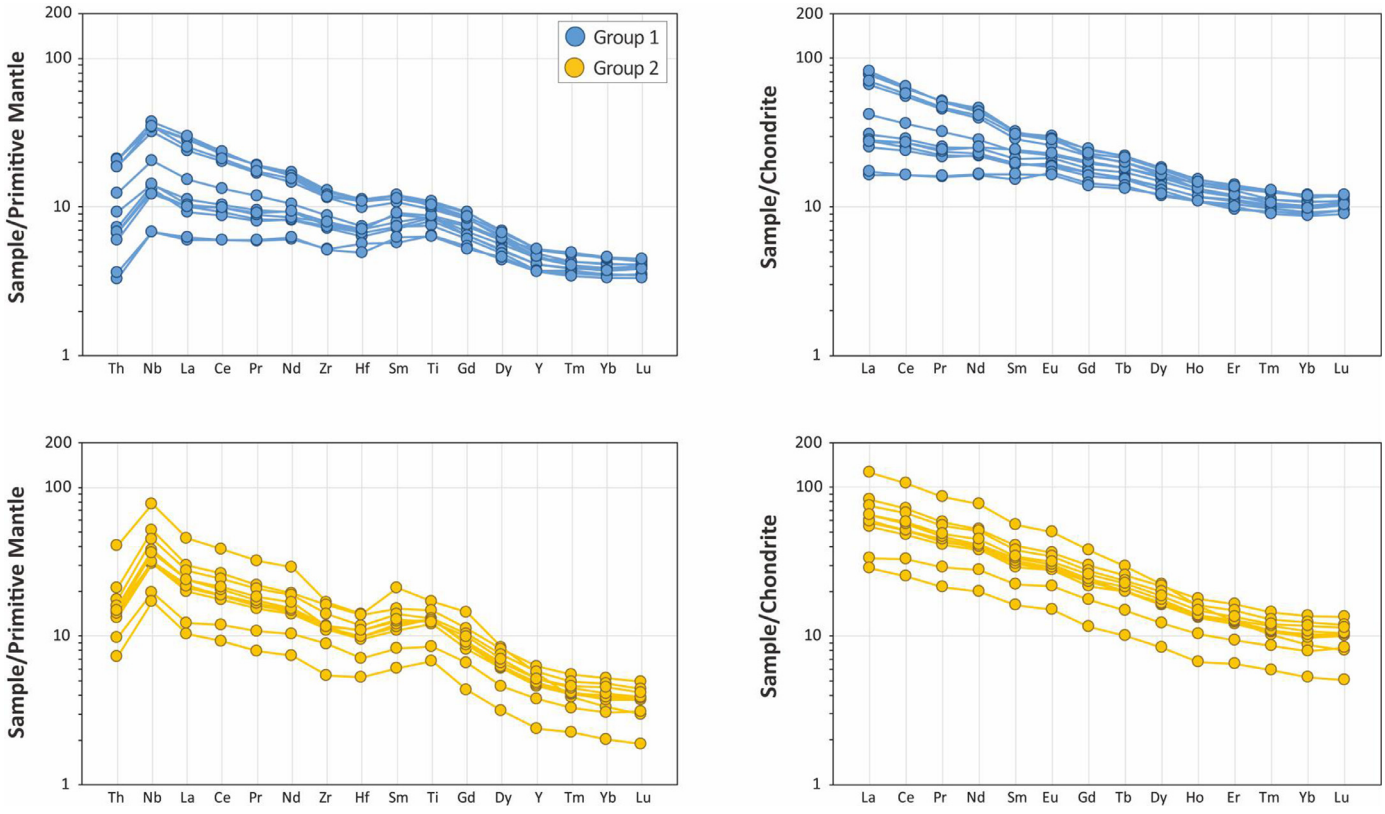

Fig. 5. Multi-element and REE patterns of the İmrahor mafic/ultramafic lithologies from the Nilüfer Unit. Normalization values are from Sun and McDonough (1989) for the chondrite, and from McDonough and Sun (1995) for the Primitive Mantle.

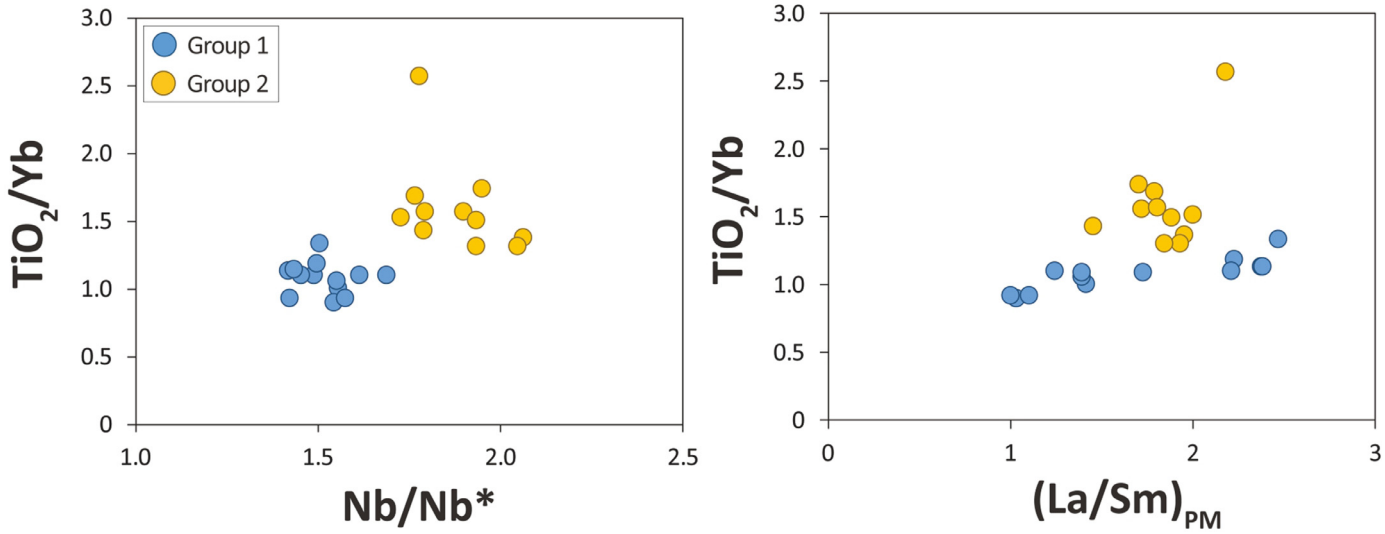

Fig. 6. Variation of TiO_2/Yb vs. Nb/Nb* and $(La/Sm)_{PM}$ for the İmrahor mafic/ultramafic lithologies from the Nilüfer Unit.

and Group 2 with Nb/Nb* between 1.73-2.07. Group 2 samples, which have higher Nb/Nb*, appears to be more enriched in TiO_2 in general (Average TiO_2 = 1.90 for Group 1 and 2.65 for Group 2; TiO_2 increases to 2.77 for the latter group if the wehrlitic cumulate sample is excluded). In addition, Group 2 samples are characterized by higher TiO_2/Yb in average (TiO_2/Yb = 1.07 for Group 1 and 1.59 for Group 2) and they show higher TiO_2/Yb values at a given La/Sm (Fig. 6). On the other hand, both groups display depleted Th/La ratios ($[Th/La]_{PM}$ = 0.55-0.90 for Group 1 and 0.62-0.89 for Group 2), with wide, but somewhat similar level of absolute LREE enrichment and fractionation ($[La/Sm]_N$ = 1.0-2.5 for Group 1 and 1.5-2.2 for Group 2; where N refers to chondrite-normalized). The two groups also exhibit varying degrees of HREE fractionation ($[Dy/Yb]_N$ = 1.3-1.7 for Group 1 and 1.5-2.6 for Group 2).

4.4. Discussion

4.4.1. Post-melting magmatic modifications

The Imrahor lithologies span a wide range in MgO, implying a role for fractional crystallization (FC)/accumulation processes in their petrogenesis. Even though there are some Mg-rich basaltic

and gabbroic samples (with ~11 wt.% MgO), none of them represent primary magmas on the basis of their Ni, Cr, and Co concentrations. The wehrlitic sample, on the other hand, is a cumulate with very high Ni and Cr content (810 and 1500 ppm, respectively), consistent with its petrography. Olivine is a major fractionating phase in the Imrahor samples, controlling the wide MgO range and correlated Ni, Cr, and Co abundances. Pyroxene is also involved in the fractionating assemblage (probably for MgO < ~8 wt.%), as reflected by the decrease in Cr and Sc with decreasing MgO. Plagioclase is another phase joining the fractionation assemblage, as indicated by the positive correlation between Al_2O_3 and MgO. Thus, the FC process appears to have significant control on the compatible element budget via the removal of ol + px + plag. In contrast, the highly incompatible elements (Th, Nb, and La) show scattered variations, and their concentrations vary widely for a given MgO, which cannot be explained by the FC process. This, instead, can depend on partial melting and/or the nature of the mantle source, which will be discussed in the following paragraphs.

4.4.2. Preliminary insights into the mantle source

Among highly incompatible trace elements, Th, Nb, and La are also fluid-immobile. Fractionation of these elements during partial melting is relatively small; thus, their ratios can be regarded to reflect that of the source (e.g., Sun and McDonough, 1989). In contrast, the ratios with elements of different compatibilities (e.g., Zr/Nb, Nb/Y) would be fractionated during low degrees of partial melting. Thus, except for high degrees of melting, the ratios of these elements do not mimic the source characteristics. However, they can still be helpful in inferring source-related features of a heterogeneous mantle and melt mixing (e.g., Niu and Batiza, 1997; Kamber and Collerson, 2000; Reiners, 2002). In a heterogeneous mantle, enriched streaks/pods (possibly in the form of pyroxenite or metasomatized peridotite) are more fusible owing to their lower solidi, compared to the depleted matrix (in the form of anhydrous peridotite; e.g., Hirschmann and Stolper, 1996). Thus, during melting of heterogeneous mantle, the low-degree melt fractions would primarily reflect geochemical signatures of the enriched component, while the high-degree melts would largely involve the characteristics of the depleted component.

As stated above, Zr/Nb ratio contains elements with different compatibilities; Nb is highly incompatible, whereas Zr is moderately incompatible. During melt extraction, this difference would lead to Nb-depleted (relative to Zr) residual mantle domains. Therefore, the depleted mantle (DM) domains, like the N-MORB source mantle (i.e., depleted MORB mantle - DMM), are characterized by high Zr/Nb ratios (e.g., 34.2 for DMM; 16.0 for PM; McDonough and Sun, 1995; Workman and Hart, 2005). Since the tapping of the DM is typically achieved through high extents of melting (in a heterogeneous mantle), the trace element ratios of the DM melts (such as N-MORBs) will resemble those of their source (Fig. 7). The Zr/Nb ratios of the Imrahor samples (3.5-12.2) are lower than those of N-MORBs (average Zr/Nb = 31.8; Sun and McDonough, 1989) but rather similar to those of OIBs and E-MORBs (average Zr/Nb = 5.8 and 8.8, respectively; Sun and McDonough, 1989). Although trace element (TE)-enriched compositions can be theoretically generated from a DM-type mantle upon small degrees of melting, such melts would be rare since the onset of DM melting is generally restricted to the shallower depths (due to the lower solidus of anhydrous peridotite). This phenomenon is well observed on the mafic lavas from the East Pacific Rise (EPR) and Iceland (e.g., Niu and Batiza, 1997; Kokfelt et al., 2006), where the low-degree melts with low Zr/Nb are associated with lower $^{143}Nd/^{144}Nd$ ratios, reflecting a greater contribution from the enriched component. Based on this, the Imrahor samples with high Zr/Nb are expected to have the largest involvement of the DM component. However, even in this case, the DM contribution would not be significant since the Zr/Nb ratios of these samples still remain low compared to the DM (Fig. 7). Instead, the Imrahor melts appear to be either dominated by the enriched component or represent diluted mixtures of the DM and enriched component.

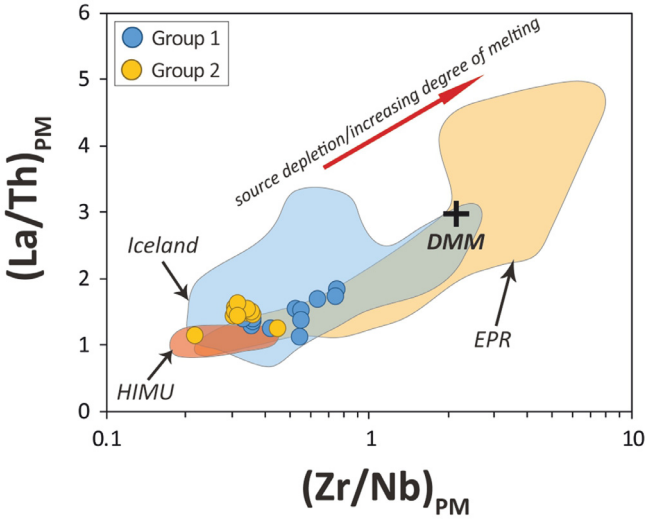

Fig. 7. $(Zr/Nb)_{PM}$ vs. $(La/Th)_{PM}$ plot of the İmrahor mafic/ultramafic lithologies from the Nilüfer Unit. Depleted MORB Mantle (DMM) from Workman and Hart (2005). Other data sources are the same as Fig. 3.

4.4.3. Melt mixing or source mixing?

The geochemistry of the oceanic basalts shows a large diversity, for which the mixing process has a critical role. Mixing may take place in the solid-state (i.e., source mixing), which is characterized by the bulk mixtures of the distinct mantle components (e.g., Hart et al., 1992). Alternatively, 'melt mixing' may occur, including the mixtures of melts from different mantle components. Although both processes are essentially some form of mixing, the chemistry of the resulting melts would be different because the concentrations of the elements in the solid and melt phases would significantly differ. If the source mixing is the primary cause of the compositional variation, then the melting of the mixed source should result in curvilinear arrays in the binary plots of elements with different incompatibilities (such as Zr and Nb). In contrast, if the heterogeneity is due to melt mixing, a linear correlation would be expected since the distribution is not controlled by the element incompatibility but becomes an equation of mixing instead (e.g., Langmuir et al., 1978; Niu and Batiza, 1997; Kamber and Collerson, 2000).

On the plot of Zr-Nb (Fig. 3), the Imrahor samples display a strong correlation, implying that melt mixing is the predominant process responsible for the observed variation, rather a solid mixing. It must be noted, however, that FC could also yield a linear trend since both Zr and Nb have low bulk partition coefficients for typical fractionating phases, such as olivine, clinopyroxene, and plagioclase during the magmatic evolution of mafic magmas. To test this, the sample compositions were corrected to 14 wt.% MgO (see Fig. 8 for details regarding the correction procedure). After correcting for fractionation, although the spread of the Zr-Nb variation decreases to some extent, the range and correlation defined by Zr and Nb still remain significant (Fig. 8). Thus, it appears that although FC may have played some role in the Zr-Nb systematics of the Imrahor samples, it cannot explain the wide and correlated Zr-Nb spectrum. This, in turn, suggests that melt mixing was an essential process creating chemical diversity in the petrogenesis of the studied lithologies.

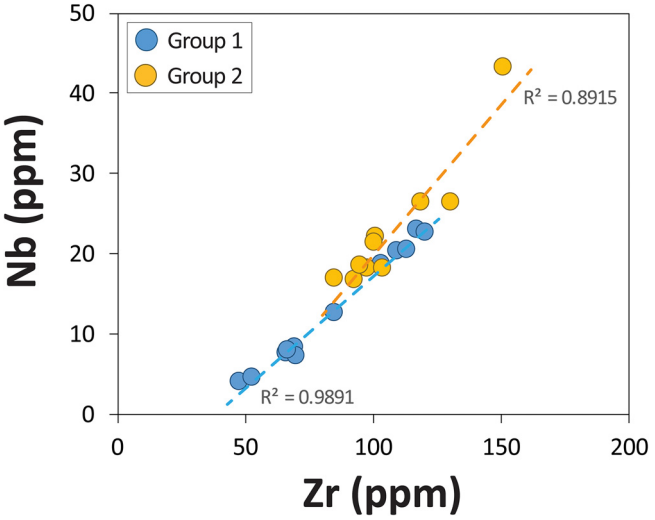

Fig. 8. Zr-Nb systematics of the İmrahor samples from the Nilüfer Unit for the assessment of melt mixing. The sample compositions were corrected to 14 wt.% MgO (arbitrarily chosen to represent a primary/parental magma composition). For the correction, a similar procedure to that of Kamber of Collerson (2000) is adopted, in which (i) 0.4 olivine (ol) + 0.2 clinopyroxene (cpx) + 0.4 plagioclase (plag) is assumed to fractionate up to 6 wt.% MgO; (ii) 0.6 ol + 0.2 cpx + 0.2 plag between 6-8 wt.% MgO; (iii) 0.6 ol + 0.4 cpx between 8-10 wt.% MgO; (iv) olivine only for > 10 wt.% MgO.

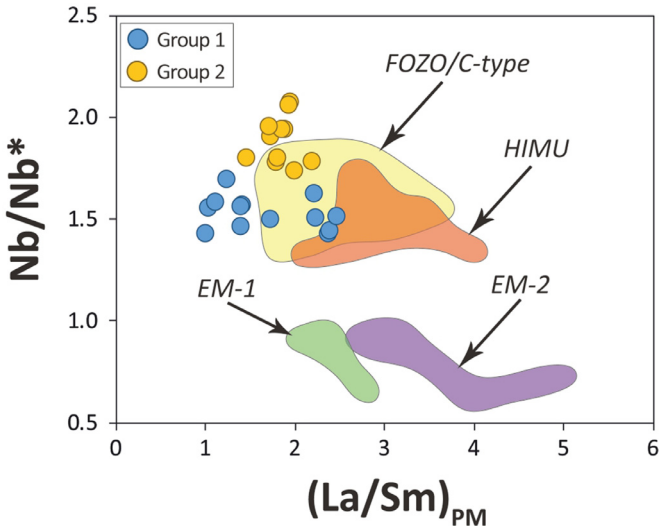

Fig. 9. $(La/Sm)_{PM}$ vs. Nb/Nb* plot of the İmrahor samples from the Nilüfer Unit. FOZO/C-, HIMU-, EM-1, and EM-2-type samples were selected on the basis of isotope compositions. FOZO/C-type samples are compiled from Mid-Atlantic Ridge 5-11°S (Hoernle et al., 2011), and 37°17' N and 37°50' N (Gale et al., 2011). East Pacific Rise (5-15°N) (Niu and Batiza, 1997), Iceland (Kokfelt et al., 2006), Walvis Ridge (Gibson et al., 2005), and Azores (Elliott et al., 2007; Waters et al., 2020). EM-1 is compiled from Walvis Ridge (Gibson et al., 2005; Salters and Sachi-Kocher, 2010), while EM-2 is from Samoa (Jackson et al., 2010).

4.4.4. Nature of the enriched end-member

The linear Zr-Nb trend indicates the involvement of at least two end-members (e.g., Kamber and Collerson, 2000). Although the mantle end-members (e.g., DM, HIMU, EM-1, etc.) have been defined on isotopic grounds, trace elements can also provide insights into the mantle components in the absence of isotopic data (e.g., Weaver, 1991; Niu and Batiza, 1997). The fluid-immobile Th-La-Nb systematics, for example, can deliver source-related information, which might be particularly critical for the petrogenesis of altered/metamorphosed rocks. Some oceanic- and continental-derived magmas possess strong enrichment in Nb relative to Th and La, thus displaying positive Nb anomalies or Nb-kick (e.g., Sun and McDonough, 1989; Jackson et al., 2008; Peters and Day, 2014). This difference can be attributed either to the type of material (e.g. recycled oceanic crust) within the source region and/or that the relative incompatibilities of Th-Nb-La are somewhat different than expected. Regardless of its origin, the 'Nb-kick' (i.e. high low Th/Nb and La/Nb) is a common feature of the HIMU- and FOZO/C-type melts (e.g., Weaver et al., 1987; Woodhead, 1996; Jackson et al., 2008; Sayit, 2013). The magnitude of Nb-kick, however, appears to be lowered or even disappear in the EM-type melts (e.g., Weaver et al., 1987; Workman et al., 2004; Salters and Sachi-Kocher, 2010). As a first-order approximation, the Imrahor samples can be suggested to be more akin to FOZO/C- and HIMU-type melts than EM-type melts (Fig. 9).

The most extreme compositions of the HIMU component are found in the Mangaia, Tubuai, and Rurutu islands (Pacific), with $^{206}Pb/^{204}Pb > 21$ (Woodhead, 1996; Chauvel et al., 1992; Hanyu et al., 2011). This component represents a somewhat homogeneous reservoir (e.g., Weaver, 1991; Woodhead, 1996), as evidenced by incompatible trace element ratios confined to a narrow interval (e.g., Woodhead, 1996; Lassiter et al., 2003; Hanyu et al., 2011). Also, all HIMU melts are highly enriched in LREE. This may suggest that the HIMU material is easily fusible, imprinting its signature on the small-degree melts. The HIMU samples from these localities possess strong Nb-kick, yet with Nb/Nb* ranging in a narrow interval (1.3-1.7). In this regard, Group 1 Imrahor samples with high La/Sm can be thought to represent relatively undiluted HIMU melts, with their similar Nb/Nb* values between 1.4-1.7. However, Group 1 samples, as a whole, display a wide range of LREE enrichment, with $(La/Sm)_{PM}$ as low as 1.0, which contrasts with the exclusively highly LREE-enriched nature of HIMU melts ($[La/Sm]_{PM}$ = 2.1-4.0; Fig. 9). This may imply that Group 1 samples have not tapped a relatively pure HIMU component in their petrogenesis.

It is also difficult to make a connection between Group 2 samples and the HIMU component because Group 2 samples display very high Nb/Nb* values (1.7-2.1), which are even more extreme than the HIMU melts (Nb/Nb* = 1.3-1.7; Fig. 9). Instead, such high values are akin to the melts tapping the FOZO/C component. In addition, in contrast to the relative homogeneity of HIMU, the FOZO/C melts exhibit a broader range of trace element ratios (e.g., Sayit, 2013). Therefore, the Nb-enriched signatures of Group 2 samples can be related to the involvement of the FOZO/C component rather than HIMU. In this regard, Group 1 samples may also have sampled the FOZO/C component as the enriched end-member instead of HIMU. Overall, the Imrahor samples have not received a substantial contribution from the HIMU component, as suggested by their broad La/Sm range and the very high Nb/Nb* (shown by Group 2). Instead, the geochemical characteristics of the Imrahor lithologies are more consistent with the involvement of the FOZO/C component in their mantle sources.

4.4.5. Origin of the enriched component

The Imrahor mafic magmatism seems to have involved variable contributions from an enriched, recycled/deep-sourced component with high Nb/Nb*. Such Nb-enriched melts are commonly believed to originate from the recycled basaltic oceanic crust (e.g., McDonough, 1991; Weaver, 1991; Woodhead, 1996). This crustal material is also widely envisioned to characterize the mantle source of ocean island basalts in the form of mantle plumes (e.g., Hofmann and White, 1982; Weaver, 1991; Sobolev et al., 2005). The idea is that deep dehydration/melting processes can variably mobilize LILE, Th, and LREE from the eclogitic slab, whereas HFSE and HREE remain relatively undisturbed (e.g., McDonough, 1991; Kogiso et al., 1997). Hence, in terms of Th-Nb-La systematics, the loss of Th and La, but retention of Nb leads oceanic crust to have a positive Nb anomaly.

Although recycled oceanic crust can develop Nb-kick via deep subduction processes, the element fractionations at shallow depths should also be considered. While Th and La are assumed to mobilize during deep subduction (McDonough, 1991; Kogiso et al., 1997), they act as fluid-mobile elements during hydrothermal and low-T alteration of the oceanic crust (i.e., during pre-subduction; e.g., Bach et al., 2003). In contrast to Th and La, the behavior of LILE, U and Pb are variable and erratic due to their mobility during both pre- and syn-subduction. Following its formation, the oceanic crust is hydrated (via interaction with seawater), and LILE can be variably added or leached from the crust. U is added, while Pb is lost (e.g., Albarede and Michard, 1989; Bach and Früh-Green, 2010). On the other hand, these elements are effectively removed from the slab during subduction. After being modified through hydration/dehydration/melting processes, the residual oceanic crust might be highly depleted in LILE, Pb, and U. Alternatively, the net result can be highly erratic, especially regarding LILE. In both cases, the resulting enrichment levels and/or elemental fractionations would contrast with those observed in OIBs and E-MORBs (e.g., Niu and O'Hara, 2003). In addition, OIBs display uniform Ce/U and Ba/Ce ratios (Halliday et al., 1995), which would be difficult to obtain when the variable mobilities of these elements are considered. Another issue to consider is the density of the subducted crust. When injected into the lower mantle, the subducted crust remains at higher densities than the surrounding mantle (e.g., Ono et al., 2001), thus being unable to rise and getting trapped somewhere in the lower mantle. Therefore, considering both chemical and physical issues, the recycled oceanic crust does not seem to be a suitable material to explain the Nb-rich, enriched end-member for the Imrahor mafic magmatism.

Another alternative to creating the Nb-kick would be melting in the deep mantle. Under lower melting conditions, trace element fractionation differs from the upper mantle due to different mineral phases. For example, Th and La, which are so-called highly incompatible elements in the upper mantle, become highly compatible in the lower mantle with the presence of Ca-perovskite (e.g., Corgne et al., 2005). Nb, on the other hand, remains to be incompatible since no lower mantle phase can strongly partition this element. Melting in the lower mantle, thus, would cause a strong decoupling between Th-La and Nb, imparting a positive Nb anomaly on the melt. However, due to the strong partitioning of U into Ca-perovskite (e.g., Corgne et al., 2005), such Nb-enriched lower mantle melts would also possess low U/Pb ratios and develop contrasting EM-type isotopic signatures instead (e.g., Collerson et al., 2010). Hence, a lower mantle origin does not seem to explain the genesis of Nb-enriched melts, with typically FOZO/C- or HIMU-type isotopic signatures rather than EM.

The metasomatized oceanic lithospheric mantle (OLM) can be thought of as another candidate. This material includes a metasomatic agent, probably in the form of very small-degree melts derived from the LVZ (e.g., Green, 1971; Sun and McDonough, 1989; Niu and O'Hara, 2003). This is well evidenced by the trace element and isotope systematics of the MORBs. When certain trace element ratios (such as Th/La and Nb/Zr, where the more incompatible element is written as the numerator) are plotted against Sr-Nd-Pb isotopic ratios, it is observed that such trace element ratios increase with increasing contribution from the isotopically enriched component (e.g., Niu and Batiza, 1997; Niu et al., 2002). This may suggest that this enrichment is controlled by melt, i.e., metasomatic agent, which is further reinforced by the uniformity of Ba/Ce and Ce/U ratios observed in OIBs (Halliday et al., 1995). Also, U being more incompatible than Ba and Rb for some OIBs may support such origin, which can be attributed to the presence of metasomatic accessory/minor phases (e.g. amphibole and phlogopite) that can partition the latter elements (Halliday et al., 1995).

4.4.6. The role of metasomatized oceanic lithospheric mantle

Metasomatized OLM seems a more suitable material to characterize the enriched component in the petrogenesis of Imrahor lithologies. This idea was also assessed here by geochemical modeling (Fig. 10). The modeling involves several steps; (i) generation of the metasomatic melt from upper mantle peridotite (in the LVZ), (ii) creation of the metasomatized peridotite (i.e., metasomatized OLM) via hybridization/mixing of the metasomatic melt and the host peridotite, (iii) melting of the metasomatized OLM (as the enriched component) and DM-type peridotite (as the depleted component), (iv) melt mixing (between metasomatized OLM and DM melts) to produce the final melt.

The Nb-enriched MORBs and OIBs show depletion in Th relative La, resulting (i.e., $[La/Th]_{PM} > 1$), a feature also existing in the Imrahor samples (Fig. 7). This depletion appears to be inherited from the source since Th and La are both highly incompatible and not greatly fractionated from each other during upper mantle melting and subduction dehydration/melting processes (e.g., Sun and McDonough, 1989; Kogiso et al., 1997). Therefore, the host mantle peridotite (unmetasomatized) can be considered with $(La/Th)_{PM} > 1$, similar to the DM. In the modeling (Fig. 10), the metasomatic melt was assumed to be generated at the LVZ within the garnet-stability field, and characterized by very small melt fractions (F = ~0.5-1%), resulting in significant incompatible element enrichment. Such small-volume LVZ melts will be volatile-rich, and can leave their source region; however, they will freeze upon reaching the base of lithosphere (Green, 1971; McKenzie, 1989).

An appealing feature of the modeling is that the calculated metasomatic melt is strongly enriched in Nb ($Nb/Nb^* = \sim 1.8\text{-}2.3$) due to $D_{Th} \approx D_{Nb} < D_{La}$. In this way, while $(La/Th)_{PM}$ ratio still remains greater than 1, a positive Nb anomaly is produced without needing an additional process (i.e., subduction). The more incompatible nature of Th and Nb (relative to La) is also evidenced by the melting systematics of MORBs and OIBs (e.g., Sun and McDonough, 1989; Niu and Batiza, 1997). The magnitude of Nb-kick depends mainly on the degree of melt fraction rather than the type of DM-type peridotite. D-DMM, DMM, and E-DMM compositions (Workman and Hart, 2005) are all relatively low in Nb/Nb^* (~1.3); therefore, the addition of small-degree metasomatic melt into these compositions would result in a positive Nb anomaly. After adding the metasomatic melt to the OLM peridotite, the resulting lithology becomes a metasomatized OLM peridotite representing the enriched component. The modeling reveals that the metasomatized OLM possesses high $(La/Th)_{PM}$, strong Nb-kick, and may have a chondritic or enriched La/Sm ratio (see Fig. 10 for the details). On the other hand, the unmetasomatized peridotitic domain surrounding metasomatized OLM may characterize the depleted component. Thus, recycled OLM can be envisioned to consist of both enriched and depleted domains.

The melt mixing process was also integrated into the modeling to produce the final melt. Both sample groups in this study can be successfully generated by the melt mixtures of the metasomatized OLM and depleted peridotite. It must be noted that metasomatized OLM starts melting earlier than anhydrous peridotite; hence it is expected to dominate the early, low-degree melt fractions. The modeling allows a significant contribution (up to 100%) from metasomatized OLM to produce highly enriched Imrahor compositions in the dataset. Lowering the metasomatized OLM proportion (e.g., 70%) can also yield successful results, but such cases require lower F for metasomatic melt and metasomatized OLM. The differences between the two groups can be explained by the melt fraction (F) of the metasomatic melt and its mass proportion in the host peridotite. Group 2 requires integration of smaller F and a relatively larger proportion in the mixture (i.e., less proportion of the host peridotite) to develop higher Nb/Nb^* ratios than Group 1. While this explains the main difference between the sample groups, the

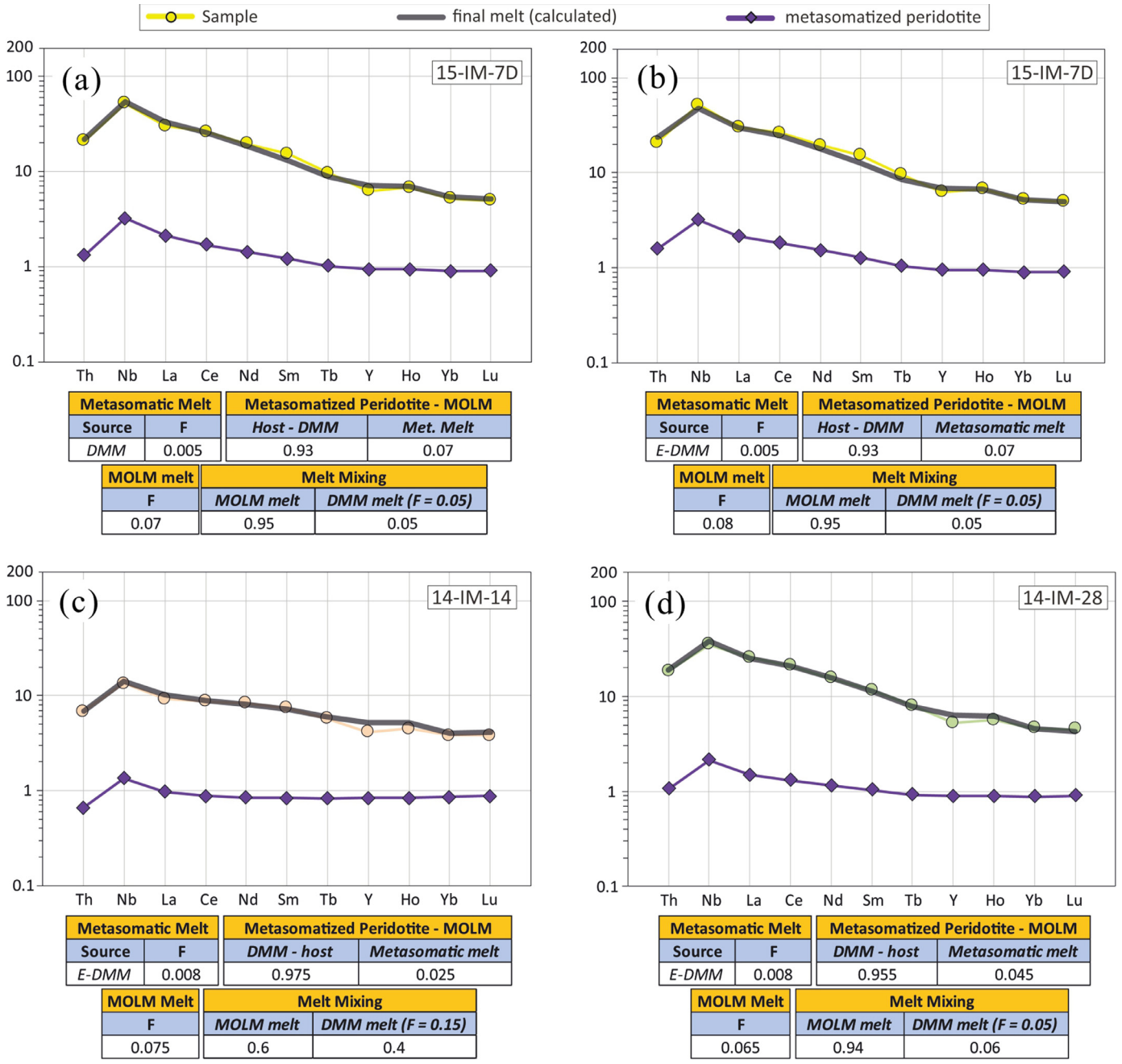

Metasomatic Melt		Metasomatized Peridotite - MOLM	
Source	F	*Host - DMM*	*Met. Melt*
DMM	0.005	0.93	0.07

MOLM melt	Melt Mixing	
F	*MOLM melt*	*DMM melt (F = 0.05)*
0.07	0.95	0.05

Metasomatic Melt		Metasomatized Peridotite - MOLM	
Source	F	*Host - DMM*	*Metasomatic melt*
E-DMM	0.005	0.93	0.07

MOLM melt	Melt Mixing	
F	*MOLM melt*	*DMM melt (F = 0.05)*
0.08	0.95	0.05

Metasomatic Melt		Metasomatized Peridotite - MOLM	
Source	F	*DMM - host*	*Metasomatic melt*
E-DMM	0.008	0.975	0.025

MOLM Melt	Melt Mixing	
F	*MOLM melt*	*DMM melt (F = 0.15)*
0.075	0.6	0.4

Metasomatic Melt		Metasomatized Peridotite - MOLM	
Source	F	*DMM - host*	*Metasomatic melt*
E-DMM	0.008	0.955	0.045

MOLM Melt	Melt Mixing	
F	*MOLM melt*	*DMM melt (F = 0.05)*
0.065	0.94	0.06

Fig. 10. Geochemical modeling for the assessment of the metasomatized oceanic lithospheric mantle (OLM) in the petrogenesis of the Imrahor samples from the Nilüfer Unit. The elements used in the modeling are selected such that they are sensitive to (i) the Nb-kick, (ii) LREE/HREE fractionation, (iii) HREE fractionation. A non-modal, batch melting scheme of Shaw (1970) was adopted. In the model, the metasomatic melt is assumed to derived from garnet peridotite. The metasomatized OLM, which represent here the Nb-enriched, FOZO/C-like mantle material, is also characterized by garnet peridotite. For this lithology, the source mode is taken as 0.60 ol + 0.20 opx + 0.14 cpx + 0.06 grt, which melts in the proportions 0.01 ol + 0.04 opx + 0.55 cpx + 0.40 grt (Haase et al., 1997). DMM-type melts, which later mixes with Nb-enriched metasomatized OLM melts, are assumed to derive from spinel peridotite. Regarding spinel peridotite, the mode is assumed to be 0.612 ol + 0.203 opx + 0.135 cpx + 0.025 sp, which melts in the proportions 0.02 ol + 0.08 opx + 0.75 cpx + 0.15 sp (Haase et al., 1997). Final produced melt (after melt mixing), is calculated after 20% olivine removal, for which Rayleigh fractionation is assumed to occur. DMM and E-DMM values are from Workman and Hart (2005). Partition coefficients are taken from Adam and Green (2006).

variations within Group 1 and Group 2 themselves need somewhat a different explanation. In the light of the modeling, more depleted compositions within each group can be explained by higher contributions from the host peridotite and DM-type melt, which would buffer the LREE enrichment.

4.4.7. A possible link to the mantle plumes?

The seismic anomalies reveal two major mantle upwellings (also called superplumes) in the lower mantle, underlying the Africa and Pacific plates. These upwellings are characterized by very low seismic anomalies, and the peripheries of these regions can be possible locations from which the mantle plumes have been derived (e.g., Burke et al., 2008). These low-velocity regions are suggested to have existed at least 300 Ma (Burke et al., 2008) and encompass both temporally and spatially the within-plate Permian-Triassic magmatism in the Tethyan realm (e.g., Pe-Piper, 1998; Al-Riyami and Robertson, 2002; Genç, 2004; Sayit et al., 2010; Maury et al., 2008; Tekin et al., 2019).

Hence, mantle plumes may have played an essential role in the Tethyan magmatism, as also suggested by several studies (e.g., Lapierre et al., 2004; Sayit and Göncüoglu, 2009; Tekin et al., 2019).

The Nb-enriched İmrahor melts (this study), as a part of the voluminous Triassic Nilüfer mafic magmatism, may have been possibly sourced from the mantle plumes within the Tethyan realm. The enriched component reflected by the İmrahor samples appears to be FOZO/C-like based on the trace element systematics. This mantle component is envisioned here to be the oceanic lithospheric mantle, which has been metasomatized by very small-degree, volatile melt fractions derived from the LVZ (e.g., Green, 1971; Frey and Green, 1974; Niu and O'Hara, 2003). Such metasomatic melts may possess high Nb/Nb* values (this study) and generate diverse geochemical signatures based on the role of accessory phases (Pilet et al., 2005). After metasomatic modification, the oceanic lithosphere would include enriched (wet metasomatized OLM) and depleted (dry OLM) domains. This lithospheric material is eventually recycled at the subduction zone, traveling down to the lower mantle (van der Hilst et al., 1997; Kellogg et al., 1999). Here, the oceanic lithosphere will probably get rid of much of its crustal part, leaving the oceanic lithospheric mantle as the predominant lithology. The Nb-enriched, FOZO/C-like signatures originate from the metasomatized OLM itself, while the EM-type characteristics can be produced by the incorporation of a small amount of crustal sedimentary material (e.g., Weaver, 1991; Jackson et al., 2007) or originate from the metasomatized OLM itself via diverse metasomatic processes (e.g., Workman et al., 2004; Pilet et al., 2005; Salters and Sachi-Kocher, 2010). After some period of residence, this material heats up and rises as a mantle plume, becoming the source of TE-enriched Tethyan magmatism, and contributing to the mantle heterogeneity. The influence of mantle plumes on the Tethyan realm appears to be a global-scale phenomenon, starting from the Dinarides (e.g., Lugovic et al., 1991; Ustaszewski et al., 2009); Albanides (e.g., Bortolotti et al., 2004; Tashko et al., 2009), Hellenides (e.g., Pe-Piper, 1998; Saccani et al., 2003a, 2003b, 2008; Photiades et al., 2003; Bortolotti et al., 2004; Monjoie et al., 2008; Koglin et al., 2009; Chiari et al., 2012), and Carpathians (Hoeck et al., 2009) in the west, and stretching up to the Middle East (e.g., Lapierre et al., 2004; Sayit and Göncüoglu, 2009; Göncüoglu et al., 2010; Saccani et al., 2013; Esmaeili et al., 2020; this study) and Tibet (e.g., Xia et al., 2008; Dai et al., 2011; Wang et al., 2019).

Declaration of interests

The authors declare that they have no known competing financial interests or personal relationships that could have appeared to influence the work reported in this paper.

Acknowledgements

I appreciate the constructive comments from the editor Emilio Saccani and two anonymous reviewers. This study was funded by METU BAP-08-11-2015-030.

Supplementary materials

Table S1. Whole-rock geochemical data of the Imrahor mafic/ultramafic lithologies from the Nilüfer Unit.

Table S2. Results of standard and replicate analyses.

Supplementary material associated with this article can be found, in the online version, at doi:10.1016/j.geogeo.2022.100139.

References

Adam, J., Green, T., 2006. Trace element partitioning between mica- and amphibole-bearing garnet-lherzolite and hydrous basanitic melt: 1. Experimental results and the investigation of controls on partitioning behavior. Contrib. Mineral. Petrol. 152, 1–17.

Albarede, F., Michard, A., 1989. Hydrothermal alteration of the oceanic crust. In: Hart, S.R., Gülen, L. (Eds.), Crust-mantle Recycling at Convergence Zones. Springer, Dordrecht, pp. 29–36.

Al-Riyami, K., Robertson, A., 2002. Mesozoic sedimentary and magmatic evolution of the Arabian continental margin, northern Syria: evidence from the Baer-Bassit Melange. Geol. Mag. 139, 395–420.

Altıner, D., Koçyiğit, A., 1993. Third remark on the geology of the Karakaya basin. An Anisian megablock in northern central Anatolia: micropaleontologic, stratigraphic and tectonic implications for the rifting stage of Karakaya basin. Turkey. Revue de Palaeobiologie 12, 1–17.

Altıner, D., Kocyigit, A., Farinacci, A., Nicosia, U., Conti, M.A., 1991. Jurassic-Lower Cretaceous stratigraphy and paleogeographic evolution of the southern part of northwestern Anatolia. Geol. Romana. 27, 13–80.

Bach, W., Früh-Green, G.L., 2010. Alteration of the oceanic lithosphere and implications for seafloor processes. Elements 6, 173–178.

Bach, W., Peucker-Ehrenbrink, Hart, S.R., Blusztajn, J.S., 2003. Geochemistry of hydrothermally altered oceanic crust: DSDP/ODP Hole 504B – implications for seawater-crust exchange budgets and Sr- and Pb-isotopic evolution of the mantle. Geochem. Geophys. Geosys. 4 (3), 8904. doi:10.1029/2002GC000419.

Bortolotti, V., Chiari, M., Kodra, A., Marcucci, M., Mustafa, F., Principi, G., Saccani, E., 2004. New evidence for Triassic MORB magmatism in the northern Mirdita Zone ophiolites (Albania). Ofioliti 29, 243–246.

Burke, K., Torsvik, T.H., 2004. Derivation of Large Igneous Provinces of the past 200 million years from long-term heterogeneities in the deep mantle. Earth Planet. Sci. Lett. 227, 531–538.

Burke, K., Steinberger, B., Torsvik, T.H., Smethurst, M.A., 2008. Plume generation zones at the margins of large low shear velocity provinces on the core-mantle boundary. Earth Planet. Sci. Lett. 265, 49–60.

Chauvel, C., Hofmann, A.W., Vidal, P., 1992. HIMU-EM: The French Polynesian connection. Earth Planet. Sci. Lett. 110, 99–119.

Chiari, M., Bortolotti, V., Marcucci, M., Photiades, A., Principi, G., Saccani, E., 2012. Radiolarian biostratigraphy and geochemistry of the Koziakas massif ophiolites (Greece). Bull. Soc. Geol. Fr. 183 (4), 287–306.

Collerson, K.D., Williams, Q., Ewart, A.E., Murphy, D.T., 2010. Origin of HIMU and EM-1 domains sampled by ocean island basalts, kimberlites and carbonatites: the role of CO2-fluxed lower mantle melting in thermochemical upwellings. Phys. Earth Planet. Inter. 181, 112–131.

Corgne, A., Liebske, C., Wood, B.J., Rubie, D.C., Frost, D.J., 2005. Silicate perovskite-melt partitioning of trace elements and geochemical signature of a deep perovskitic reservoir. Geochim. Cosmochim. Acta 69, 485–496.

Dai, J., Wang, C., Hébert, R., Li, Y., Zhong, H., Guillaume, R., Bezard, R., Wei, Y., 2011. Late Devonian OIB alkaline gabbro in the Yarlung Zangbo Suture Zone: remnants of the Paleo-Tethys? Gondwana Res 19, 232–243.

Elliott, T., Blichert-Toft, J., Heumann, A., Koetsier, G., Forjaz, V., 2007. The origin of enriched mantle beneath São Miguel, Azores. Geochim. Cosmochim. Acta. 71, 219–240.

Esmaeili, R., Xiao, W., Ebrahimi, M., Zhang, J., Zhang, Z., El-Rahman, A., Han, C., Wan, B., Ao, S., Song, D., Shahabi, S., Aouizerat, A., 2020. Makran ophiolitic basalts (SE Iran) record Late Cretaceous Neotethys plume-ridge interaction. Int. Geol. Rev. 62, 1677–1697.

Eyuboglu, Y., Dudas, F.O., Chatterjee, N., Santosh, M., Billor, M.Z., Yuva, S., 2018. Petrology, geochronology and tectonic setting of Early Triassic alkaline metagabbros from the eastern Pontide orogenic belt (NE Turkey): implications for the geodynamic evolution of Gondwana's early Mesozoic northern margin. Tectonics 37, 3174–3206.

Festa, A., Pini, G.A., Dilek, Y., Codegone, G., 2010. Mélanges and mélange-forming processes: a historical overview and new concepts. Int. Geol. Rev. doi:10.1080/00206810903557704.

Frey, F.A., Green, D.H., 1974. The mineralogy, geochemistry and origin of lherzolite inclusions in Victorian basanites. Geochim. Cosmochim. Acta. 38, 1023–1059.

Gale, A., Escrig, S., Gier, E.J., Langmuir, C.H., Goldstein, S.L., 2011. Enriched basalts at segment centers: the Lucky Strike (37°17'N) and Menez Gwen (37°50'N) segments of the Mid-Atlantic Ridge. Geochem. Geophys. Geosys. 12, Q06016. doi:10.1029/2010GC003446.

Genç, Ş.C., 2004. A Triassic large igneous province in the Pontides, northern Turkey: geochemical data for its tectonic setting. J. Asian of Earth Sci. 22, 503–516.

Gibson, S.A., Thompson, R.N., Day, J.A., Humphris, S.E., Dickin, A.P., 2005. Melt-generation processes associated with the Tristan mantle plume: Constraints on the origin of EM-1. Earth Planet. Sci. Lett. 237, 744–767.

Göncüoglu, M.C., 2018. Geology. In: Kapur, S., Akça, E., Günal, H. (Eds.), The Soils of Turkey. Springer, Cham, pp. 57–73.

Göncüoglu, M.C., 2019. A review of the geology and geodynamic evolution of tectonic terranes in Turkey. In: Pirajno, F., Ünlü, T, Dönmez, C., Şahin, M. (Eds.), Mineral Resources of Turkey. Springer, Cham, pp. 19–72.

Göncüoglu, M.C., Sayit, K., Tekin, U.K., 2010. Oceanization of the northern Neotethys: Geochemical evidence from ophiolitic melange basalts within the İzmir–Ankara suture belt, NW Turkey. Lithos 116, 175–187.

Göncüoglu, M.C., Dirik, K., Kozlu, H., 1997. Pre-Alpine and alpine terranes in Turkey: Explanatory notes to the terrane map of Turkey. Ann. Géol. de Pays Hell. 37, 515–536.

Green, D.H., 1971. Compositions of basaltic magmas as indicators of conditions of origin: application to oceanic volcanism. Philos. Trans. R. Soc. Lond. A 268, 707–725.

Haase, K.M., Stoffers, P., Garbe-Schönberg, C.D., 1997. The petrogenetic evolution of lavas from Easter Island and neighbouring seamounts, near-ridge hotspot volcanoes in the SE Pacific. J. Petrol. 6, 785–813.
Halliday, A.N., Lee, D-C., Tommasini, S., Davies, G.R., Paslick, C.R., Fitton, J.G., James, D.E., 1995. Incompatible trace elements in OIB and MORB and source enrichment in the sub-oceanic mantle. Earth Planet. Sci. Lett. 133, 379–395.
Hanan, B.B., Graham, D.W., 1996. Lead and helium isotope evidence from oceanic basalts for a common deep source of mantle plumes. Science 272, 991–995.
Hanyu, T., Tatsumi, Y., Senda, R., Miyazaki, T., Chang, Q, Hirahara, Y., Takahashi, T., Kawabata, Suzuki, Kimura, J-I., 2011. Geochemical characteristics and origin of the HIMU reservoir. A possible mantle plume source in the lower mantle. Geochem. Geophys. Geosys. 12, Q0AC09. doi:10.1029/2010GC003252.
Hart, S.R., Hauri, E.H., Oschmann, L.A., Whitehead, J.A., 1992. Mantle plumes and entrainment: isotopic evidence. Science 256, 517–520.
Hirschmann, M.M., Stolper, E.M., 1996. A possible role for garnet pyroxenite in the origin of the "garnet signature" in MORB. Contrib. Mineral. Petrol. 124, 185–208.
Hoeck, V., Ionescu, C., Balintoni, I., Koller, F., 2009. The Eastern Carpathians "ophiolites" (Romania): Remnants of a Triassic ocean. Lithos 108, 151–171.
Hoernle, K., Hauff, F., Kokfelt, T.F., Haase, K., Garbe-Schönberg, D., Werner, R., 2011. On and off-axis chemical heterogeneities along the South Atlantic Mid-Ocean-Ridge (5–11° S): shallow or deep recycling of ocean crust and/or intraplate volcanism? Earth Planet. Sci. Lett. 306, 86–97.
Hofmann, A.W., White, W.M., 1982. Mantle plumes from ancient oceanic crust. Earth Planet. Sci. Lett. 57, 421–436.
Jackson, M.G., Hart, S.R., Saal, A., Schimizu, N., Kurz, M.D., Blusztajn, J.S., Skovgaard, A.C., 2008. Globally elevated titanium, tantalum, and niobium (TITAN) in ocean island basalts with high $^{3}He/^{4}He$. Geochem. Geophys. Geosys. 9, Q04027. doi:10.1029/2007GC001876.
Jackson, M.G., Hart, S.R., Koppers, A.A.P., Staudigel, H., Konter, J., Blusztajn, J., Kurz, M., Russell, J.A., 2007. The return of subducted continental crust in Samoan lavas. Nature 448, 684–687.
Jackson, M.G., Hart, S.R., Konter, J.G., Koppers, A.A.P., Staudigel, H., Kurz, M.D., Blusztajn, J., Sinton, J.M., 2010. Samoan hot spot track on a "hot spot highway": implications for mantle plumes and a deep Samoan mantle source. Geochem. Geophys. Geosys. 11, Q12009. doi:10.1029/2010GC003232.
Kamber, B., Collerson, K.D., 2000. Zr/Nb systematics of ocean island basalts reassessed – the case for binary mixing. J. Petrol. 41, 1007–1021.
Kaya, O., Mostler, H., 1992. A Middle Triassic age for low-grade greenschist facies metamorphic sequence in Bergama (İzmir), western Turkey: the first paleontological age assignment and structural-stratigraphic implications. Newslett. Stratigr. 26, 1–17.
Kellogg, L.H., Hager, B.H., van der Hilst, R.D., 1999. Compositional stratification in the deep mantle. Science 283, 1881–1884.
Koçyiğit, A., 1991. An example of accretionary forearc basin from Central Anatolia and its implications of subduction of Neo-Tethys in Turkey. Geol. Soc. Am. Bull. 103, 22–36.
Kogiso, T., Tatsumi, Y., Nakano, S., 1997. Trace element transport during dehydration processes in the subducted oceanic crust: 1. Experiments and implications for the origin of ocean island basalts. Earth Planet. Sci. Lett. 148, 193–205.
Koglin, N., Kostopoulos, D., Reischmann, T., 2009. Geochemistry, petrogenesis and tectonic setting of the Samothraki mafic suite, NE Greece: Trace-element, isotopic and zircon age constraints. Tectonophysics 473, 53–68.
Kokfelt, T.M., Hoernle, K., Hauff, F., Fiebig, J., Werner, R., Garbe-Schönberg, D., 2006. Combined trace element and Pb-Nd-Sr-O isotope evidence for recycled oceanic crust (upper and lower) in the Iceland mantle plume. J. Petrol. 47, 1705–1749.
Langmuir, C.H., Vocke Jr, R.D., Hanson, G.N., 1978. A general mixing equation with applications to Icelandic basalts. Earth Planet. Sci. Lett. 37, 380–392.
Lapierre, H., Samper, A., Bosch, D., Maury, R.C., Béchennec, F., Cotten, J., Demant, A., Brunet, P., Keller, F., Marcoux, J., 2004. The Tethyan plume: geochemical diversity of Middle Permian basalts from the Oman rifted margin. Lithos 74, 167–198.
Lassiter, J.C., Blichert-Toft, J., Hauri, E.H., Barsczus, H.G., 2003. Isotope and trace element variations in lavas from Raivavae and Rapa, Cook-Austral islands: constraints on the nature of HIMU- and EM-mantle and the origin of mid-plate volcanism in French Polynesia. Chem. Geol. 202, 115–138.
Lugovic, B., Altherr, R., Raczek, I., Hofmann, A.W, Majer, V., 1991. Geochemistry of peridotites and mafic igneous rocks from the Central Dinaric Ophiolite Belt, Yugoslavia. Contrib. Mineral. Petrol. 106 (2), 201–216.
Marroni, M., Göncüoglu, M.C., Frassi, C., Sayit, K., Pandolfi, L., Ellero, A., Ottria, G., 2020. The Intra-Pontide ophiolites in Northern Turkey revisited: from birth to death of a Neotethyan oceanic domain. Geosci. Front. 11, 129–149.
Maury, R.C., Lapierre, H., Bosch, D., Marcoux, J., Krystyn, L., Cotton, J., Bussy, F., Brunet, P., Senebier, F., 2008. The alkaline intraplate volcanism of the Antalya nappes (Turkey): a Late Triassic remnant of the Neotethys. Bull. Soc. Geol. Fr. 179, 397–410.
McDonough, W.F., 1991. Partial melting of subducted oceanic crust and isolation of its residual eclogitic lithology. Philos. Trans. Royal Soc. Lond. A 335, 407–418.
McDonough, W.F., Sun, S.-s., 1995. The composition of the Earth. Chem. Geol. 120, 223–253.
McKenzie, D., 1989. Some remarks on the movement of small melt fractions in the mantle. Earth Planet. Sci. Lett. 95, 53–72.
McKenzie, D., O'Nions, R.K., 1983. Mantle reservoirs and ocean island basalts. Nature 301, 229–231.
Monjoie, P., Lapierre, H., Tashko, A., Mascle, G.H., Dechamp, A., Muceku, B., Brunet, P., 2008. Nature and origin of the Triassic volcanism in Albania and Othrys: a key to understanding the Neotethys opening? Bull. Soc. Geol. Fr. 179, 411–425.
Niu, Y., Batiza, R., 1997. Trace element evidence from seamounts for recycled oceanic crust in the Eastern Pacific mantle. Earth Planet. Sci. Lett. 148, 471–483.
Niu, Y., O'Hara, M.J., 2003. Origin of ocean island basalts: A new perspective from petrology, geochemistry, and mineral physics considerations. J. Geophys. Res. 108 (B4), 2209. doi:10.1029/2002JB002048.
Niu, Y., Regelous, M., Wendt, I.J., Batiza, R., O'Hara, M.J., 2002. Geochemistry of near-EPR seamounts: importance of source vs. process and the origin of enriched mantle component. Earth Planet. Sci. Lett. 199, 327–345.
Okay, A.I., 2000. Was the Late Triassic orogeny in Turkey caused by the collision of an oceanic plateau? In: Bozkurt, E., Winchester, J., Piper, J.A. (Eds.) Tectonics and magmatism in Turkey and the Surrounding Area. Geol. Soc. Lond. Spec. Publ, pp. 139–161 173.
Okay, A.İ., Göncüoglu, M.C., 2004. The Karakaya complex: a review of data and concepts. Turk. J. Earth Sci. 13, 77–95.
Ono, S., Ito, E., Katsura, T., 2001. Mineralogy of subducted basaltic crust (MORB) from 25 to 37 GPa, and chemical heterogeneity of the lower mantle. Earth Planet. Sci. Lett. 190, 57–63.
Parlak, O., Robertson, A., 2004. The ophiolite-related Mersin Melange, southern Turkey: its role in the tectonic-sedimentary setting of Tethys in the Eastern Mediterranean region. Geol. Mag. 141, 257–286.
Pearce, J.A., 1975. Basalt geochemistry used to investigate past tectonic environments on Cyprus. Tectonophysics 25, 41–67.
Pe-Piper, G., 1998. The nature of Triassic extension-related magmatism in Greece: evidence from Nd and Pb isotope geochemistry. Geol. Mag. 135, 331–348.
Peters, B.J., Day, J.M.D., 2014. Assessment of relative Ti, Ta, and Nb (TITAN) enrichments in oceanic island basalts. Geochem. Geophys. Geosys. 15, 4424–4444.
Pickett, E.A., Robertson, A.H.F., 1996. Formation of the Late Palaeozoic–Early Mesozoic Karakaya Complex and related ophiolites in NW Turkey by Palaeotethyan subduction–accretion. J. Geol. Soc. 153, 995–1009.
Pilet, S., Hernandez, J., Sylvester, P., Poujol, M., 2005. The metasomatic alternative for ocean island basalt chemical heterogeneity. Earth Planet. Sci. Lett. 236, 148–166.
Photiades, A., Saccani, E., Tassinari, R., 2003. Petrogenesis and tectonic setting of volcanic rocks from the Subpelagonian ophiolitic mélange in the Agoriani area (Othrys, Greece). Ofioliti 28, 121–135.
Reiners, P.W., 2002. Temporal-compositional trends in intraplate basalt eruptions: implications for mantle heterogeneity and melting processes. Geochem. Geophys. Geosys. 3 (2). doi:10.1029/2001GC000250.
Saccani, E., Padoa, E., Photiades, A., 2003a. Triassic mid-ocean ridge basalts from the Argolis Peninsula (Greece): new constraints for the early oceanization phases of the Neo-Tethyan Pindos basin. In: Dilek, Y., Robinson, P.T., eds. Geol. Soc. London Sp. Publ., 218, 109-127.
Saccani, E., Photiades, A., Padoa, E., 2003b. Geochemistry, petrogenesis and tectono–magmatic significance of volcanic and subvolcanic rocks from the Koziakas Mélange (Western Thessaly, Greece). Ofioliti 28, 43–57.
Saccani, E., Photiades, A., Santato, A., Zeda, O., 2008. New evidence for supra-subduction zone ophiolites in the Vardar zone from the Vermion massif (northern Greece): Implication for the tectono-magmatic evolution of the Vardar oceanic basin. Ofioliti 33, 65–85.
Saccani, E., Azimzadeh, Z., Dilek, Y., Jahangiri, A., 2013. Geochronology and petrology of the Early Carboniferous Misho Mafic Complex (NW Iran), and implications for the melt evolution of Paleo-Tethyan rifting in Western Cimmeria. Lithos 162-163, 264–278.
Saccani, E., Delavari, M., Dolati, A., Marroni, M., Pandolfi, L., Chiari, M., Barbero, 2018. New insights into the geodynamics of Neo-Tethys in the Makran area: Evidence from age and petrology of ophiolites from the Coloured Mélange Complex (SE Iran). Gondwana Res 62, 306–327.
Salters, J.M., Sachi-Kocher, A., 2010. An ancient metasomatic source for the Walvis Ridge basalts. Chem. Geol. 273, 151–167.
Sayit, K., 2013. Immobile trace element systematics of ocean island basalts: the role of oceanic lithosphere in creating the geochemical diversity. Ofioliti 38 (1), 101–120.
Sayit, K., Göncüoglu, M.C., 2009. Geochemistry of mafic rocks of the Karakaya complex, Turkey: evidence for plume involvement in the Palaeotethyan extensional regime during the Middle and Late Triassic. Int. J. Earth Sci. 98, 367–385.
Sayit, K., Göncüoglu, M.C., 2013. Geodynamic evolution of the Karakaya Mélange Complex, Turkey: a review of geological and petrological constraints. J. Geodyn. 65, 56–65.
Sayit, K., Göncüoglu, M.C., Furman, T., 2010. Petrological reconstruction of Triassic seamounts/oceanic islands within the Palaeotethys: Geochemical implications from the Karakaya subduction/accretion Complex, Northern Turkey. Lithos 119, 501–511.
Sayit, K., Tekin, U.K., Göncüoglu, M.C., 2011. Early-middle Carnian radiolarian cherts within the Eymir Unit, Central Turkey: Constraints for the age of the Palaeotethyan Karakaya Complex. J. Asian Earth Sci. 42, 398–407.
Sayit, K., Bedi, Y., Tekin, U.K., Göncüoglu, M.C., Okuyucu, C., 2017. Middle Triassic back-arc basalts from the blocks in the Mersin Mélange, southern Turkey: Implications for the geodynamic evolution of the Northern Neotethys. Lithos 268-271, 102–113.
Shaw, D.M., 1970. Trace element fractionation during anatexis. Geochim. Cosmochim. Acta 34, 237–243.
Shervais, J.W., 2006. The significance of subduction-related accretionary complexes in early Earth processes. In: Reimold, W.U., Gibson, R.L. (Eds.), Processes on the Early Earth. Geol. Soc. Am. Spec, pp. 173–192 Paper 405.
Şengör, A.M.C., Yılmaz, Y., 1981. Tethyan Evolution of Turkey: a plate tectonic approach. Tectonophysics 75, 181–241.

Sobolev, A.V., Hofmann, A.W., Sobolev, S.V., Nikogosian, I.G., 2005. An olivine-free mantle source of Hawaiian shield basalts. Nature 434, 590–597.
Sun, S.-S., McDonough, W.F., 1989. Chemical and isotopic systematics of oceanic basalts: implications for mantle composition and processes. In: Saunders, A.D., Norry, M.J. (Eds.), Magmatism in the Ocean Basins. Geol. Soc. Lond. Spec. Publ, pp. 313–345 42.
Tashko, A., Mascle, G.H., Muceku, B., Lappierre, H., 2009. Nd, Pb isotope and trace element signatures of the Triassic volcanism in Albania. The relationship to the NeoTethys opening. Albanian J. Nat. Tech. Sci. 1, 3–23.
Tekin, U.K., Okuyucu, C., Sayit, K., Bedi, Y., Noble, P.J., Krystyn, L., Göncüoglu, M.C., 2019. Integrated Radiolaria, benthic foraminifera and conodont biochronology of the pelagic Permian blocks/tectonic slices and geochemistry of associated volcanic rocks from the Mersin Melange, southern Turkey: Implications for the Permian evolution of the northern Neotethys. Island Arc 28, 1–36 e12286.
Ustaszewski, K., Schmid, S.M., Lugovic, B., Schuster, R., Schaltegger, U., Bernoulli, D., Hottinger, L., Kounov, A., Fügenschuh, B., Schefer, S., 2009. Late Cretaceous intra-oceanic magmatism in the internal Dinarides (northern Bosnia and Herzegovina): Implications for the collision of the Adriatic and European plates. Lithos 108, 106–125. doi:10.1016/j.lithos.2008.09.010.
van der Hilst, R.D., Widiyantoro, S., Engdahl, E.R., 1997. Evidence for deep mantle circulation from global tomography. Nature 386, 578–584.
Xia, B., Chen, G-W, Wang, R., Wang, Q., 2008. Seamount volcanism associated with the Xigaze ophiolite, Southern Tibet. J. Asian Earth Sci. 32, 396–405.
Wang, B., Xie, C-M., Fan, J-J., Wang, M., Yu, Y-P., Dong, Y-C., Hao, Y-J., 2019. Genesis and tectonic setting of Middle Permian OIB-type mafic rocks in the Sumdo area, southern Lhasa terrane. Lithos 324-325, 429–438.
Warren, J.M., 2016. Global variations in abyssal peridotite compositions. Lithos 248-251, 193–219.
Waters, C.L., Day, J.M.D., Watanabe, S., Sayit, K., Zanon, V., Olson, K.M., Hanan, B.B., Widom, E., 2020. Sulfide mantle source heterogeneity recorded in basaltic lavas from the Azores. Geochim. Cosmochim. Acta 268, 422–445.
Weaver, B.L., 1991. The origin of ocean island basalt end-member compositions: trace element and isotopic constraints. Earth Planet. Sci. Lett. 104, 381–397.
Weaver, B.L., Wood, D.A., Tarney, J., Joron, J.L., 1987. Geochemistry of ocean island basalts from the South Atlantic: Ascension, Bouvet, St. Helena, Gough and Tristan da Cunha. Geol. Soc. Lond. Spec. Publ. 30, 253–267.
Wilson, M., Guiraud, R., 1998. Late Permian to recent magmatic activity on the African-Arabian margin of Tethys. In: Macgregor, D.S., Moody, R.T.J., Clark-Jones, D.D. (Eds.), Petroleum Geology of North Africa. Geol. Soc. Lond. Spec. Publ, pp. 231–263 132.
Winchester, J.A., Floyd, P.A., 1977. Geochemical discrimination of different magma series and their differentiation products using immobile elements. Chem. Geol. 20, 325–343.
Woodhead, J.D., 1996. Extreme HIMU in an oceanic setting: the geochemistry of Mangaia Island (Polynesia), and temporal evolution of the Cook-Austral hotspot. J. Volcanol. Geoth. Res. 72, 1–19.
Workman, R.K., Hart, S.R., 2005. Major and trace element composition of the depleted MORB mantle (DMM). Earth Planet. Sci. Lett. 231, 53–72.
Workman, R.K., Hart, S.R., Jackson, M., Regelous, M., Farley, K.A., Blusztajn, J., Kurz, M., Staudigel, H., 2004. Recycled metasomatized lithosphere as the origin of the Enriched Mantle II (EM2) end-member: evidence from the Samoan Volcanic Chain. Geochem. Geophys. Geosys. 5, Q04008. doi:10.1029/2003GC000623.
Zindler, A., Hart, S., 1986. Chemical geodynamics. Ann. Rev. Earth Planet. Sci. 14, 493–571.